THE EFFECTS OF MOS LAYERS ON SENSING PROPERTIES OF MOS PHOTOSENSOR

Wagah F. Mohammed[1], Mohammed M. Ali[2], Munther N. Al-Tikriti[3], Kalid Kaleel[4]
1&4- College of Electronics Engineering, Mosul University, Mosul, Iraq.
2 &3-Faculty of Engineering, Philadelphia University, Amman, Jordan
1. wagahfaljubori @ yahoo.com, 2. moh_19592002@yahoo.co.uk,
3. munther_baker44 @ yahoo.co.uk, 4. Kalid.kaleel@yahoo.com

Submitted: Mar. 22, 2013 ***Accepted: Apr. 30, 2013*** ***Published: June 5, 2013***

Abstract- *In this research work, many samples of metal –oxide –silicon photosensors were laboratory prepared by thermal evaporation techniques. Some silicon samples were left in the air for a predefined time for SiO_2 to grow naturally, while others were thermally coated with measured thickness of SiO. A number of the samples were coated with nickel while others with aluminum and one sample was coated with indium. Various tests and measurements were conducted; these include transmittance tests with a range of wavelength and for different thicknesses. The ideality factors of the samples and the potential barrier height were calculated from I-V and C-V characteristics. The photogenerated current of the samples were also measured at photoconductive mode under reverse voltage. Quantum efficiency measurement indicated that native oxide samples provided higher quantum efficiency than those thermally deposited samples. Detectivity measurement showed that thermally deposited oxide samples had low detectivity as compared to native oxide samples*

Index terms*:* Schottky Barrier Diode, Photosensor, MOS Photosensor, Silicon Photosensor:

I. INTRODUCTION

Artificial vision is the simulation of human vision using sensors devices that can sense visible ultraviolet and infrared lights with wavelength in range between 0.4 μm and 0.7μm.The principle of photosensor operation is basically the interaction between incident photon energy and the sensor materials. There are many types of semiconductors photosensor, homo junction, hetero junction and Schottky barrier photosensor. Schottky barrier photosensor is a metal- semiconductors junction, which has gained much attention in recent years, due to its unique properties [1, 2]. It is used for ultraviolet and vacuum ultraviolet due to its outstanding stable performance even under heavy radiant exposure [3]. A typical application of Schottky barriers photosensor is in position sensitive detector, where fast response times and high signal to noise ratio ($>10^5$) are essential. However, high photovoltaic efficiency conversion is relatively not very important [4].

Schottky hypothesis [5] for metal – semiconductor junction states that a depletion region is formed between metal and semiconductor, which is free from mobile carries. This condition can really be considered as an ideal state. But in actual application there are numerous discrepancies between the ideal state and practical state. These discrepancies include space charge region, energy band diagram and their effect on the potential barrier, the depletion region width and reverse leakage current [6,7]. The main causes for the low performance of Schottky diodes arise, essentially, from the fact that the level of reverse current is higher than in PN diodes due to thermal simulation [8]. Reverse and leakage currents are, usually, called the dark current in Schottky barrier diode. They are generated due to small Schottky barriers that are formed between the metal and semiconductor. In order to enhance the barrier height and reduce the dark current, a very thin interfacial layer can be inserted in the junction as part of the semiconductor layer [9, 10]. Consequently, high potential barrier can be obtained indicating that the thin interfacial layer had modified the barrier height by influencing the space charge region of the semiconductor layer [4]. However, the responsivity of these devices is low as result of impedance mismatch between the air-metal semiconductor system and a significant portion of the incident optical radiation reflection [11]. Transparent low resistivity metals and thin interfacial layer could enhance the potential barrier height and the sensor responsivity.

Many samples of Schottky photosensors have been prepared on silicon wafer. A very thin layer of oxide has been added between the metal and the semiconductor. Different types of metal with different thicknesses have been thermally deposited. All samples have been subjected to extensive

investigation to determine the effect of oxide layer and metals on the sensing properties of the devices. Optical and electronics properties had been studied previously [9, 12]. In this research work the structure and behavioral properties of these sensors will be investigated. This will include the effect of the interfacial layers on the reverse current and barrier height.

II. THEORETICAL BACKGROUND AND ANALYSIS

Schottky potential barrier are usually formed between metal and semiconductor to prevent electrons movement from the semiconductor to the metal as shown in figure 1. Schottky potential barrier ($Ø_B$) can be expressed mathematically as follows: [13]

$$Ø_B = Ø_m - \chi \qquad \ldots\ldots (1)$$

Where $Ø_m$ is the metal work function, χ is the semiconductor electron affinity. The built-in potential V_{bi} of semiconductor is a function of $Ø_B$ and can be expressed as:

$$V_{bi} = Ø_B - Ø_n \qquad \ldots\ldots (2)$$

Where, $Ø_n$ is the difference between conduction band (E_c) and Fermi level (E_F) in the semiconductor. Applying positive voltage on the semiconductor relative to the metal will increase the height of the potential barrier. This is known as the case of reverse biasing.

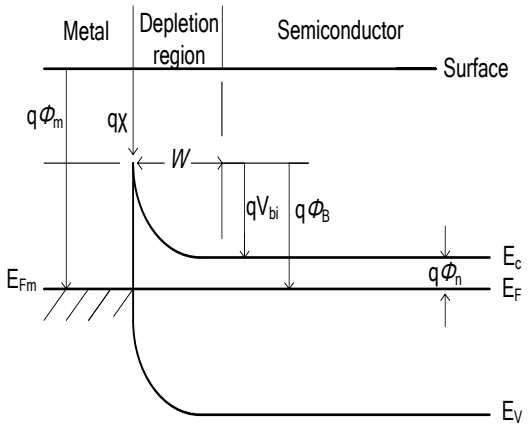

Figure 1: Ideal energy band diagram of Schottky barrier photodiode.

Table 1: The prepared samples of different structures with 100 ^{o}A metals thickness

Sample	Structure	Ideality Factor (η)	Potential Barrier (V)
D1	Ni – Si	2.50	0.69
D2	Ni –SiO_2 – Si	2.70	0.71
D3	Ni – SiO - Si	2.80	0.76
D4	Al – Si	1.50	0.79
D5	Al –SiO_2 – Si	1.67	0.81
D6	Al –SiO – Si	2.00	0.83
D7	In – SiO_2 - Si		

Schottky device operates in two different modes. The first mode is as photovoltaic, where an output current is generated due to incident light. Movements across the junction produce an

output voltage between the device terminals. This is what is commonly known as solar cell. Practical applications have shown that Schottky devices provide poor photovoltaic performance as a result of high leakage current. On the other hand the second mode of operation is the photoconductive mode which is a consequence of the application of reverse voltage across the device. The total current passing through the device is the combination of dark and photo generated currents. The positive aspects of applying reverse voltage are to increase the depletion region width, which consequently reduces the capacitance of the device and enhances responsivity and detectivity. The device capacitance C can be related to applied voltage V as follows:

$$\frac{1}{C^2} = \frac{2(V_{bi}-V)}{q\epsilon_s N_D} \quad \text{---------- (3)}$$

Where q is the electronic charge, ϵ_s is the spaces permittivity of the semiconductor and N_D is the donor carrier concentration. The capacitance represents the capacitance of depletion region in Schottky photodiode. In ordinary diode this capacitance is the diffusion capacitance which does not exist in Schottky photodiode and explains why it has very high response. The equivalent circuit of Schottky photodiode for small signal has a resistance R_{sh}, which represents the resistance of depletion region, connected in parallel with the depletion capacitance. The combination of depletion resistance and depletion capacitance is connected in series with R_s the series resistance. R_s include the connection resistance and resistance of the semiconductor bulk. The presence of series resistance makes the determination of the ideality factor and the reverse saturation current difficult. These two parameters are directly related in the identification of the potential barrier. Ideality factor, series resistance and reverse saturation current have been calculated using various methods [14]. It must be noted that the reverse leakage current will have significant importance on the reverse biasing and cannot be neglected. The current can be determined using the following equation:

$$\frac{\frac{d^2V}{dI^2}}{\left(\frac{dV}{dI}-R_s\right)^2} = \frac{q}{\eta kT}\left[1 - \frac{1}{R_{sh}}\left(\frac{dV}{dI} - R_s\right)\right] \quad \text{---------- (4)}$$

Where, η is the ideality factor, k Boltzmann constant, T the absolute temperature and R_{sh} reverse leakage resistance. R_{sh} and η can be deduced from the intersection of the curve with x-axis and y-axis respectively.

I-V characteristics for shallow layer Schottky photosensor has been explained and calculated [12, 15]. The study of these characteristics shows the existence of three regions, accumulation, depletion and inversion regions.

The increase of the mobile charges concentration on the surface separating the semiconductor and the metal will lead to increase the width of the depletion region, which in turn reduces the capacitance of the photosensor to its minimum value and consequently increases the response speed. The minimum value of depletion region capacitance can be calculated according to the following equation [16]:

$$C_{min} = \left[\frac{1}{C_{ox}} + \frac{W}{\epsilon_s}\right]^{-1} \qquad \text{---------- (5)}$$

Where, C_{ox} is the oxide capacitance and W the width of depletion region.

The application of a reverse voltage equal to the flat band voltage will result in the cancellation of the effect of the difference between the work function and electron affinity on one hand and the effect of surface charge on the other hand; this will increase the speed the photosensor response. The fabrication of high response and high signal to noise ratio Schottky photosensor will require the placement of metal thin film with high permittivity and the highest potential barrier with the least surface resistance. The semiconductor must possess high optical absorption coefficient and the depletion region should be sufficiently thick so as to have minimum capacitance.

III. SCHOTTKY PHOTOSENSORS PREPARATION AND MEASUREMENTS

The substrate was n^+- polysilicon of 355-395 μm in thickness doped with arsenic (As) in order to produce very low resistivity (around 0.005 Ω-cm) suitable for ohmic contact. The substrate was then coated with a thin layer of silicon doped with phosphors (P) to produce n-type that has resistivity in range 0.16-0.2 Ω-cm. An aluminum layer of 0.2 μm thickness was deposited on the back surface of n^+ silicon wafer to form the ohmic bulk contact of the device. Other metallic layers were deposited on the top of the oxide to form the window layer and front contact. Three types of different metals were used namely, nickel, aluminum and indium. The thickness of metals varied and the thickness of 100 A^0 was chosen so as to provide high permittivity, low surface resistance and optimized potential barrier. The annealing process was carried out at 350 ^{0}C under vacuum of 10^{-6} bar for one hour for all samples in order to support the formation of back contact. The coated substrates were thoroughly cleaned and cut to 1 cm^2 segments and left in the air for native oxide

(SiO_2) to grow. All samples prepared in this research for different parameters are listed in table 1. The samples were circular and of 0.2 cm^2 area.

Two types of measurements were performed. Dark measurements were conducted to obtain the I-V and C-V characteristics. I-V characteristics were used to identify the rectification process and the current transportation mechanism. A modern LCR meter was used to obtain the C-V characteristics. From C-V characteristics potential barriers were calculated at 10 kHz and 100 kHz frequencies. The potential barrier height was also measured for all the samples. Light measurements were also carried out in order to calculate quantum efficiency, detectivity and to plot the C- Reverse voltage characteristics.

IV. RESULTS AND DISCUSSION

Figure 2 shows the variation of transmittance with wave length for the different metals used in the samples namely nickel, aluminum and indium and for different metal thickness respectively.

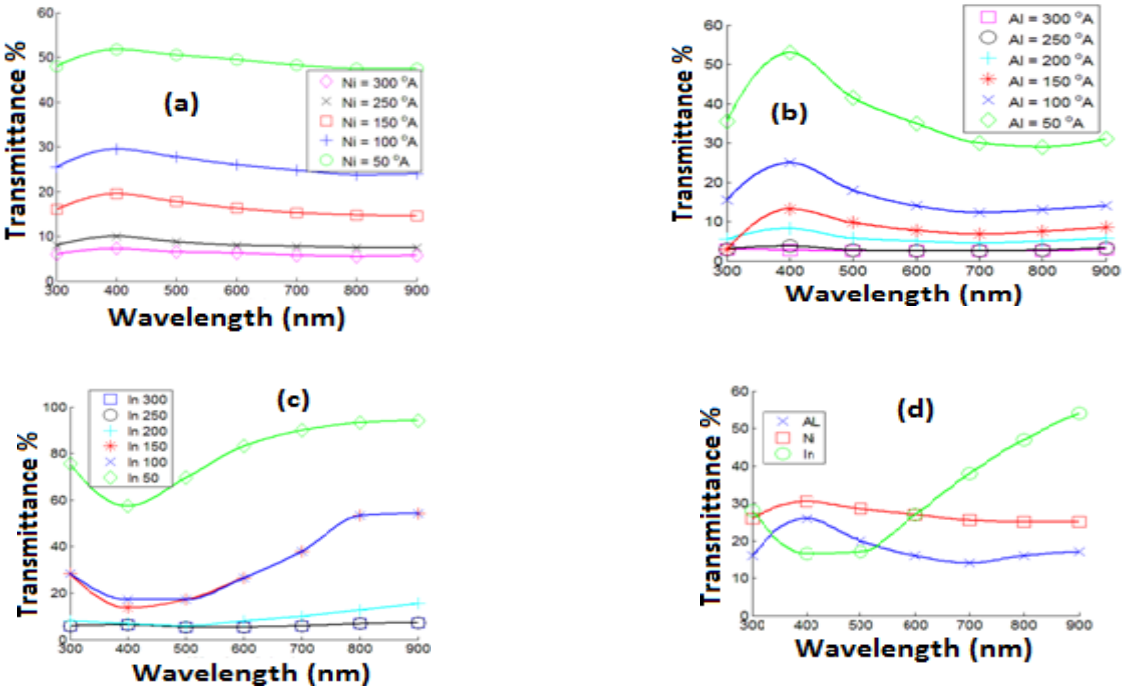

Figure 2: Variation of light transmittance with wavelength for: (a) nickel (b) aluminum, (c) indium, (d) All metals at 100 ^{o}A.

Nickel transmittance was high and almost constant throughout the wavelength range taken. Aluminum exhibited higher transmittance at 400nm wave length, while indium showed minimum transmittance at this wavelength. 100 ^{o}A metal thicknesses of the different metals were

considered. The transmittance versus wavelength were plotted for 100 ^{o}A metals thickness and shown in (figure 2-d). Indium exhibited lowest transmittance, while nickel produced the highest transmittance at short wavelength (around 400nm).

The focus of this work is on the development of optical properties of the Schottky barrier photosensor at long wavelengths. Indium metal had been extensively studied; hence this paper will concentrate on the use of nickel and aluminum as a window layer for the Schottky barrier photosensor. Figure 3(a and b) shows the I-V characteristics curves for the nickel samples (D1, D2 and D3) in addition to aluminum samples (D4, D5 and D6) with different SiO thickness respectively. The thickness of silicon oxide (sample D3 and D6) is varied in order to study the instability exhibited in these samples. It was found that the samples of minimum SiO thickness (around 36 ^{o}A for nickel and around 23 ^{o}A for aluminum samples) exhibited better stability of electronic properties.

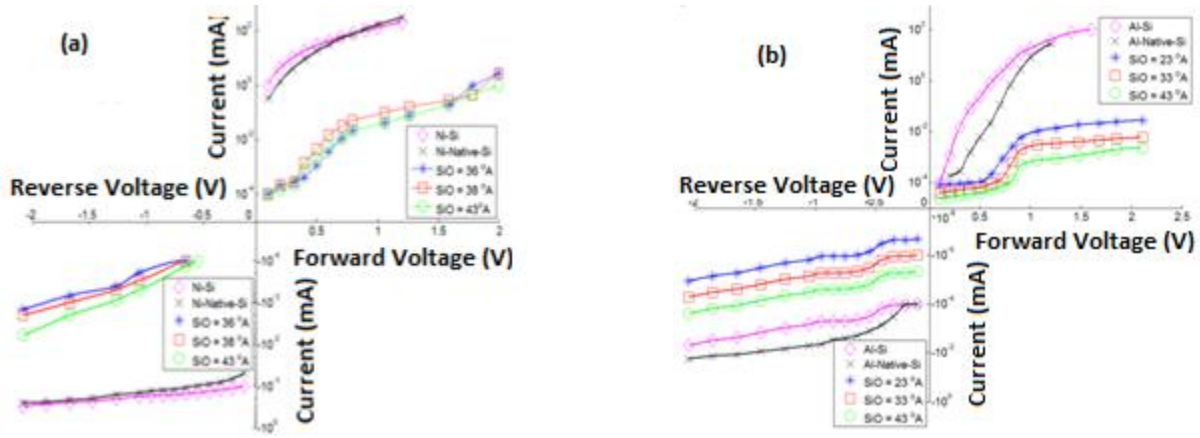

Figure 3: I–V characteristics of: (a) nickel samples D1, D2 and D3 (b) aluminum samples D4, D5 and D6, for different SiO thickness.

It can be noted from the study of the I-V characteristics curves, that while the forward currents increase with the increase in voltage, the reverse currents on the other hand remain virtually constant. Consequently, it can be stated that the potential barrier formed causes the current to be rectified. The forward current reaches near saturation level when the forward voltage exceeds 0.5 Volts. This is due to the effect of the series resistance, whose effect will appear at high values current [17]. Figure (3a and 3b) has a notable difference which is mainly, that the reverse current in aluminum does not exhibit saturation especially when SiO oxide is used. This fact is due to the reduction of the potential barrier height. These aspects will be dealt with fully later on.It would

be very beneficial to calculate some important electronic parameters such as ideality factor that can assist to identify the current transportation mechanism. This factor can be calculated from the following equation:

$$\frac{d\ln I}{dV} = \frac{q}{\eta KT} \qquad \text{---------- (6)}$$

Where, $\frac{d\ln I}{dV}$ is the slope of the curve *lnI* versus V and it is shown in figure 4a and 4b. Values of ideality factor are calculated and tabulated for linear part of the curves in table 1. For sample D1, D2 and D3 the ideality factors were 2.5, 2.7 and 2.8 respectively. It can be deduced from these results and for this range of voltages of linear parts of the curves, that the current transportation mechanism is the recombination at the surface between the metal and the semiconductor. The ideality factor is higher for sample D2 and D3 as result of lower potential barrier height due to the oxide formation. It can also be noted that the ideality factors for aluminum samples are lower than that for nickel samples. The calculated ideality factors indicate the current transportation mechanism follows the four stages discussed previously [12]. The increase of the current with the decrease in the thickness of the oxide is due tunneling effect and reduction in potential barrier.

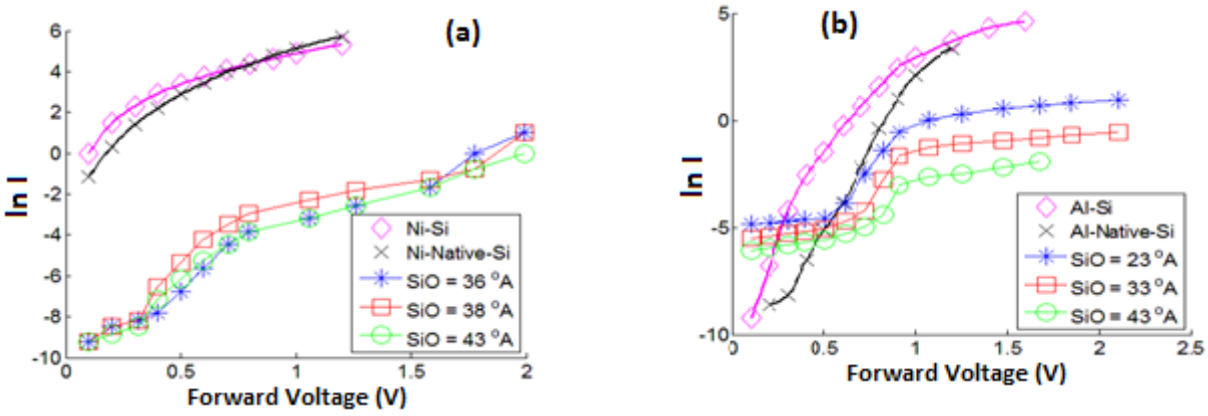

Figure 4: ln I–V characteristics of: (a) nickel samples D1, D2 and D3, (b) aluminum samples D4, D5 and D6, for different SiO thickness.

The variation of dark current and photogenerated current as function of reverse voltage for nickel and aluminum samples under two different light intensities are shown in figure 5 (a and b). The increase in the values of the revere voltage leads to the increase in the width of the depletion region which increases the absorption of photons. This will, consequently, provide higher sharing

for generated carriers which increases the value of the photogenerated current. Many measurements have been carried out for different light intensities. It has been noted that the photogenerated current increases as result of any increase in the reverse voltage at low light intensity, but when light intensity is high, the photogenerated current tends to reach saturation state. For sample D3 and D6, the current variation is affected by the reverse voltage rather than the variation of light intensity. It will increase almost linearly with the increase in the reverse voltage and does not exhibit saturation. The explanation for this is due to instability of these photosensors that causes instability of dark current which reduces their response to any variation of the light intensity. Comparison of figures 5a and 5b shows that the photogenerated current in nickel samples is higher than that of aluminum samples. These results could indicate that the density of interfacial states in nickel samples is high in comparison with the low density of interfacial states in aluminum samples.

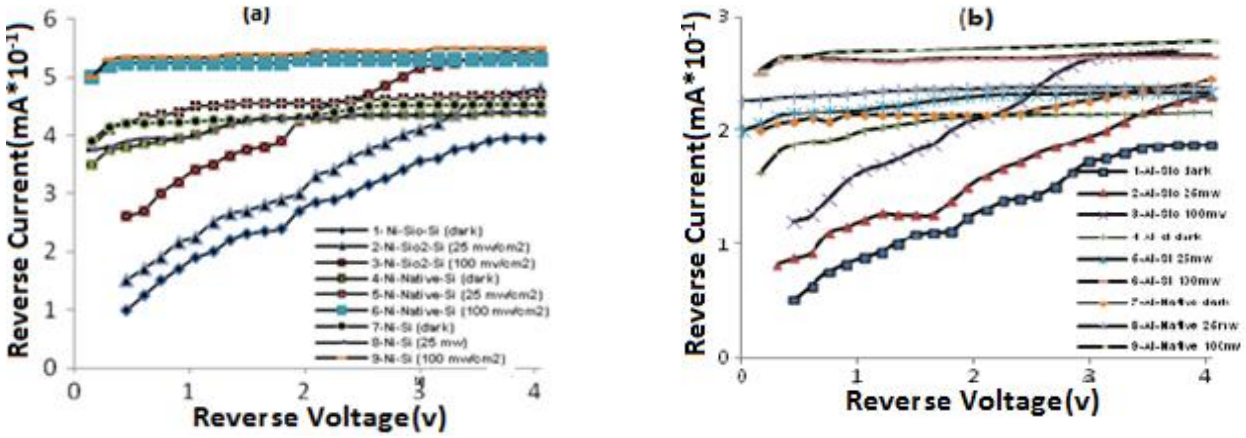

Figure 5: I – Reverse voltage characteristics of: (a) nickel samples D1, D2 and D3 (b) aluminum samples D4, D5 and D6 for dark and under two different light intensities.

The C-V characteristics for nickel and aluminum samples at 10 and 100 kHz frequencies were drawn as shown in figure 6 (a and b).. These characteristics were used to calculate the internal potential barrier height. At 10 kHz three regions were clearly apparent [12]. A recombination region appeared when the forward voltage is above 0.5V. The inversion region is associated with reverse voltage. The depletion region appeared between the two voltages mentioned. The depletion layer width is proportional with the applied voltage according to equations (3 &5). This explains why the capacitance increases linearly with the applied voltage on the depletion region that reduces the width of the region. Nickel and aluminum samples have different behavior, which, is namely the capacitance of aluminum samples increases more rapidly than for the nickel

samples. Also the capacitance decreases with the increase in frequency. The use of the photosensor at very high frequencies causes the mobile charges in the inversion region to be unable to follow the fast changes of the signal, hence the capacitance of the semiconductor will be equal to the capacitance of the depletion region and it will be almost constant at a minimum value. The time constant of minority carries generated in the inversion region will decrease with the increase in frequency.

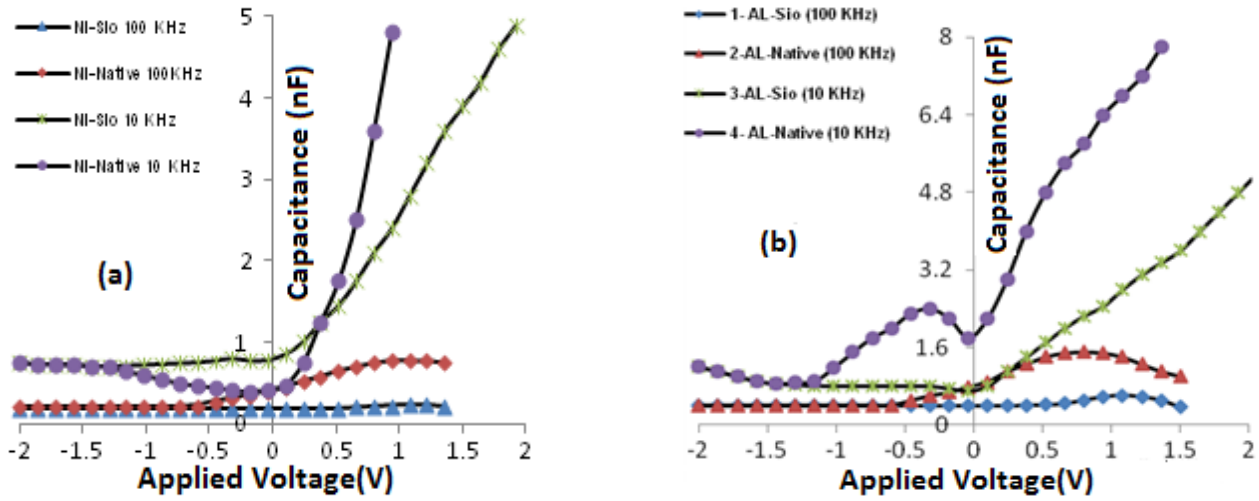

Figure 6: C–V characteristics of: (a) nickel samples D2 and D3, (b) aluminum samples D5 and D6, at 10 and 100 kHz frequency.

Using equation (3) and figure 7 which, shows the variation of V versus $\{1/C^2\}$ measured at 10 kHz, potential barrier height and carrier concentration (N_D) can be evaluated. On the other hand the ideality factors for nickel samples are higher than that for aluminum samples. Also the potential barrier in aluminum samples is higher than that for nickel samples. Again these results confirm the effect of interfacial state density difference between nickel and aluminum. These results highlight the fact that an in-depth study is needed to thoroughly address them.

The C-Reverse voltage characteristics for sample D2 for various light intensities and at 100 kHz frequency are shown in figure8. It can be deduced that the capacitance is virtually constant at dark measurement which shows that the junction is in the inversion region. When the voltage is higher than -0.5 V the capacitances increase as the light intensity increases. The capacitance decreases with the increase in frequency (see figure 8) but the opposite occurs when the light intensity increases causes the capacitance to increase. The generation of electron-hole pair will increase in relation to increase in light intensity. This reduces the surface potential barrier that

results in reduction of space charge region and increases in the value of the capacitance. When the reverse voltage becomes more negative than -0.5V, the capacitance decreases and becomes less than the dark capacitance.

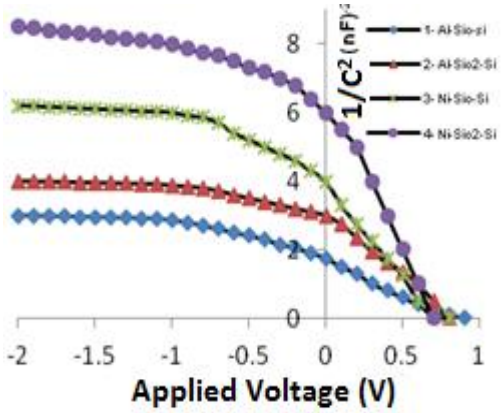

Figure 7: variation of applied voltage verses $\{1/C^2\}$ of nickel and aluminum at 10 kHz frequency.

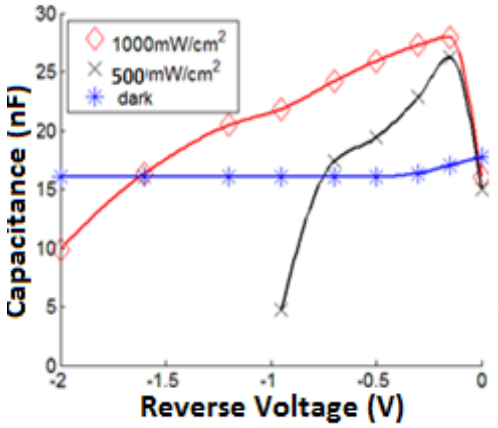

Figure 8: C- Reverse voltage characteristics for sample D2 for three light intensities and at 100 kHz frequency.

Quantum efficiency of the photosensor is defined as the number of electron-hole pairs generated. There are two types: internal (γ) which is the number of electron- hole pairs generated resulting from the absorbed photons or external (ζ) which represents the number of photons generated due to the incident photons and given by:

$$\zeta = \left[\frac{I_{ph}}{P}\right]\left[\frac{hc}{q\lambda}\right] = \alpha\,(1-\delta) \quad \text{---------- (7)}$$

Where, P is the power of light at λ wavelength, I_{ph} is the photogenerated current, h is plank constant, c light velocity, q is the electronic charge, α is the absorption coefficient and δ is the loss coefficient. It can be noted that the quantum efficiency is a function of the incident wavelengths and the material absorption coefficient. In order to maximize the absorption coefficient, the depletion region must be sufficiently wide. Figure 9 shows the plot of the quantum efficiency of some nickel and aluminum samples at variable wavelengths under 2 V of reverse voltage. It can be deduced that the samples Ni-Si and Ni-Native–Si have maximum quantum efficiency at around 450 nm wavelength. When the wavelength increases, the quantum efficiency starts to drop to low values after 900 nm wavelength. Sample Ni-SiO-Si has very low quantum efficiency. Aluminum samples exhibits lower quantum efficiency than nickel samples.

Finally, detectivity (D) of the photosensor is considered and measured for some of the samples. The expression of the detectivity is [18]:

$$D = \frac{\eta\lambda}{2hc\left(\frac{j_d}{q}\right)^{\frac{1}{2}}} \quad \text{---------- (8)}$$

Where j_d is the normalization constant related to the area of the sensor and the frequency band width of the measurements. For samples D 1, D2, D4, D5 and D6, figure 10 shows how the detectivity varies as a function of the wavelengths at 2 V reverse voltage. The detectivity increases with the increase of the wavelength and exhibits two maxima. First maximum occurs at around 500 nm wavelength, which is due to the absorbed incident photons at the surface and not from the effect of the electric field in the space charge region. The second maximum occurs at around1µm wavelength due to the increase in the optical absorption depth at longer wavelength i.e. band to band absorption. The highest detectivity is shown by samples D5 at approximately $3.25X10^{10}$ cm/Hz W at around 500 nm wavelength, while the lowest detectivity is shown by sample D6 due to high leakage current. Hence, the leakage current can be considered as mostly noise current which leads to reduction in detectivity.

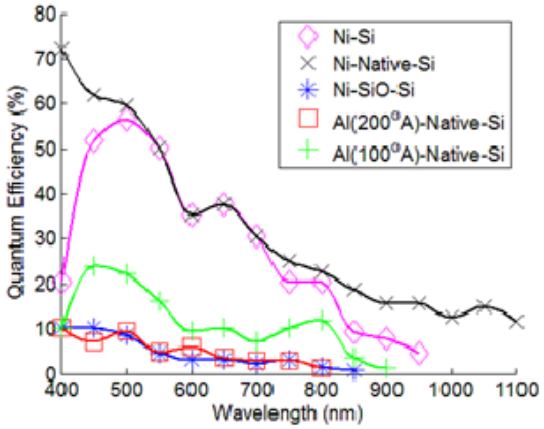

Figure 9: Quantum efficiency for different wavelength at 2V of reverse voltages for samples D1, D2, D3 and D5.

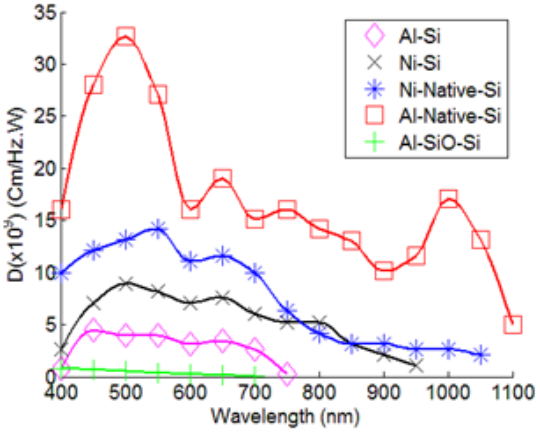

Figure 10: Detectivity varies as a function of the wave length at 2V reverse voltage for samples D1, D2, D4, D5 and D6

V. CONCLUSIONS

High speed photosensors are used in fiber-optic communication receivers, optical data links and sampling systems. In these applications, the Schottky photosensor is required to have high quality properties such as high bandwidth, high responsivity and low dark current. In order that the

photosensor exhibits these properties, Schottky structure must have high potential barrier, high transmittivity, small ideality factor, low surface resistance in addition to narrower depletion region and small body capacitance. The transmittivity and the surface resistance parameters can be controlled by changing the type and thickness of the metal. Nickel samples possess high and constant transmittivity, while aluminum samples are more stable. The results have indicated that the nickel samples have higher interfacial states as compared to aluminum samples. With the introduction of thin oxide layer between the semiconductor and the metal, it has been proven that the photosensorors with native oxide exhibit adequate ideality factor, potential barrier and lower dark current by comparison with thermally deposited oxide layer which produces high dark current and have unstable response.

ACKNOWLEDGMENT

The authors would like to acknowledge with appreciation the technical support of Mosul University. Grateful thanks also to Suzanne Munther Al-Tikriti for typing the full text of the manuscript.

REFERENCES

[1] K. Slot and H. Melchior," PtSi(n)–Si(p) Schottky-barrier photo detectors with stable spectral responsivity in the 120–250 nm spectral range", Appl. Phys. Lett., Vol. 69(24), (1996), pp. 3662.

[2] H. A ´ Guas, E. Fortunato and R. Martins," Role of the i layer surface properties on the performance of a-Si: H Schottky barrier photodiodes", Sensors and Actuators, Vol. A-99 (2002), pp. 220–223.

[3] M. Razeghi and A. Rogalski," Semiconductor ultraviolet detectors", J. Appl. Phys., Vol. 79, (1996), pp.7433; http://dx.doi.org/10.1063/1.362677.

[4] C. Yu and H. Wang," Large lateral photovoltaic effect in metal-oxide-semiconductor structures", Sensors, Vol. 10, (2010), pp. 10155-10180; doi: 10.3390/s101110155.

[5] S. M. Sze," Physics of semiconductor devices", 3rd Edition, ISBN: 978-0-471-14323-9, John Wiley and Sons, (2006).

[6] G. S. Louie and M. L. Cohen, "Electronic structure of a metal-semiconductor interface", Phys. Rev. Vol. B 13, (1976), pp. 2461–2469.

[7] S. J. Fonash, "Theory of capacitance and conductance behavior of Schottky-barrier and conducting M-I-S diodes with interface traps" J. Appl. Phys. , Vol. 48 (9), (1977), pp.3957.

[8] E. Fortunato, R. Martins and J.L. Sears, "Properties of Amorphous Silicon and its Alloys, EMIS DATA Review Series, (1998), pp. 273.

[9] W. F. Mohamad, A. AbuHajar and A. N. Saleh, "Effect of oxide layers and metals on photoelectric and optical properties of Schottky barrier photo detector", Renewable Energy, Vol. 31 (10), (2006), pp. 1493 -1498.

[10] O. Güllü, Ş. Aydoğanb and A. Türüt," High barrier Schottky diode with organic interlayer" Solid State Communications, Vol. 152, (2012), pp. 381–385.

[11] W. A. Wohlmuth, J. W. Seo, P. Fay, C. Caneau and I. Adesida, "A high-speed ITO–InAlAs–InGaAs Schottky barrier photo detector", IEEE Photonics Technology Letters, Vol. 9, No. 10, (1997), pp. 1388.

[12] W. F. Mohammad and N. N. Khatib, "Investigations of currents mechanisms and electronic properties of Schottky barrier diode" i-manager's Journal on Electronics Engineering, Vol. 2, No. 3, pp. 30- 36, March – May 2012.

[13] B. L. Sharma, "Metal--semiconductor Schottky barrier junctions and their applications", Plenum Press, (1984), pp. 370.

[14] S. Aazou and E. M. Assaid, "Schottky diode parameters extraction using two different methods**"** , International Conference on Microelectronics (ICM), Morocco, (2009).

[15] Y. L. Hao, A. P. Djotyan, A. A. Avetisyan and F. M. Peeters ," Shallow donor states near a semiconductor-insulator-metal interface" Physical Review B, Vol. 80, No. 3, (2009), PP. 10.

[16] H. C. Card and E. H. Rhoderick," Studies of tunnel MOS diodes: Thermal equilibrium considerations" J. Appl. Phys, Vol. 4, No. 10, (1971), PP. 1602.

[17] Wagah F. Mohammad, O. Daoud and Munther Al-Tikriti, "Power conversion enhancement of CdS/CdTe solar cell interconnected with tunnel diode", Circuits and Systems Journal, Vol. 3, No. 3, California, USA (2012).

[18] D. Shen, S. T. Kowel and C. A. Eldering "Amorphous silicon thin-film photodetectors for optical interconnection" Optical Engineering, Vol. 34(03), (1995), PP. 881-886.